AD-A095 382 ARMY MISSILE COMMAND REDSTONE ARSENAL AL ADVANCED S--ETC F/G 17/9
IMPACT OF SYSTEM ERRORS ON TMR PROCESSING.(U)
JAN 81 A W RIHACZEK

UNCLASSIFIED DRSMI-RE-CR-81-7 SBIE-AD-E950 090 NL

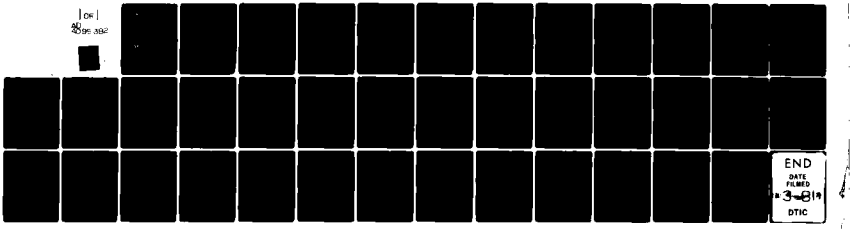

END
DATE FILED
3-81
DTIC

TECHNICAL REPORT RE-CR-81-7

IMPACT OF SYSTEM ERRORS ON TMR PROCESSING

August W. Rihaczek
Mark Resources, Inc.
Marina Del Ray, California 90291

1 January 1981

Approved for public release; distribution unlimited.

U.S. ARMY MISSILE COMMAND
Redstone Arsenal, Alabama 35809

DISPOSITION INSTRUCTIONS

WHEN THIS REPORT IS NO LONGER NEEDED, DEPARTMENT OF THE ARMY ORGANIZATIONS WILL DESTROY IT IN ACCORDANCE WITH THE PROCEDURES GIVEN IN AR 380-5.

DISCLAIMER

THE FINDINGS IN THIS REPORT ARE NOT TO BE CONSTRUED AS AN OFFICIAL DEPARTMENT OF THE ARMY POSITION *UNLESS SO DESIG*-NATED BY OTHER AUTHORIZED DOCUMENTS.

TRADE NAMES

USE OF TRADE NAMES OR MANUFACTURERS IN THIS REPORT DOES NOT CONSTITUTE AN OFFICIAL INDORSEMENT OR APPROVAL OF THE USE OF SUCH COMMERCIAL HARDWARE OR SOFTWARE.

SECURITY CLASSIFICATION OF THIS PAGE (When Data Entered)

REPORT DOCUMENTATION PAGE	READ INSTRUCTIONS BEFORE COMPLETING FORM
1. REPORT NUMBER: TR-RE-CR-81-7 / 2. GOVT ACCESSION NO.: AD-A095382	3. RECIPIENT'S CATALOG NUMBER: 2
4. TITLE (and Subtitle): Impact of System Errors on TMR Processing	5. TYPE OF REPORT & PERIOD COVERED: Final Technical Report
	6. PERFORMING ORG. REPORT NUMBER
7. AUTHOR(s): August W. Rihaczek	8. CONTRACT OR GRANT NUMBER(s): N/A
9. PERFORMING ORGANIZATION NAME AND ADDRESS: Mark Resources, Inc. Marina Del Ray, California 90291	10. PROGRAM ELEMENT, PROJECT, TASK AREA & WORK UNIT NUMBERS
11. CONTROLLING OFFICE NAME AND ADDRESS: US Army Missile Command ATTN: DRSMI-RPT Redstone Arsenal, AL 35809	12. REPORT DATE: 1 Jan 1981 13. NUMBER OF PAGES
14. MONITORING AGENCY NAME & ADDRESS(if different from Controlling Office): Commander US Army Missile Command ATTN: DRSMI-RE Redstone Arsenal, AL 35809	15. SECURITY CLASS. (of this report): UNCLASSIFIED 15a. DECLASSIFICATION/DOWNGRADING SCHEDULE
16. DISTRIBUTION STATEMENT (of this Report): Approved for public release; Distribution unlimited.	
17. DISTRIBUTION STATEMENT (of the abstract entered in Block 20, if different from Report)	
18. SUPPLEMENTARY NOTES	
19. KEY WORDS (Continue on reverse side if necessary and identify by block number): TMR Processing; Oscillator Stability; Amplifier Noise; System Timing	
20. ABSTRACT (Continue on reverse side if necessary and identify by block number): This report addresses the question of what requirements are placed on the hardware quality in order to provide adequate capabilities when using target motion resolution (TMR) techniques in a realistic environment.	

DD FORM 1 JAN 73 1473 EDITION OF 1 NOV 65 IS OBSOLETE

SECURITY CLASSIFICATION OF THIS PAGE (When Data Entered)

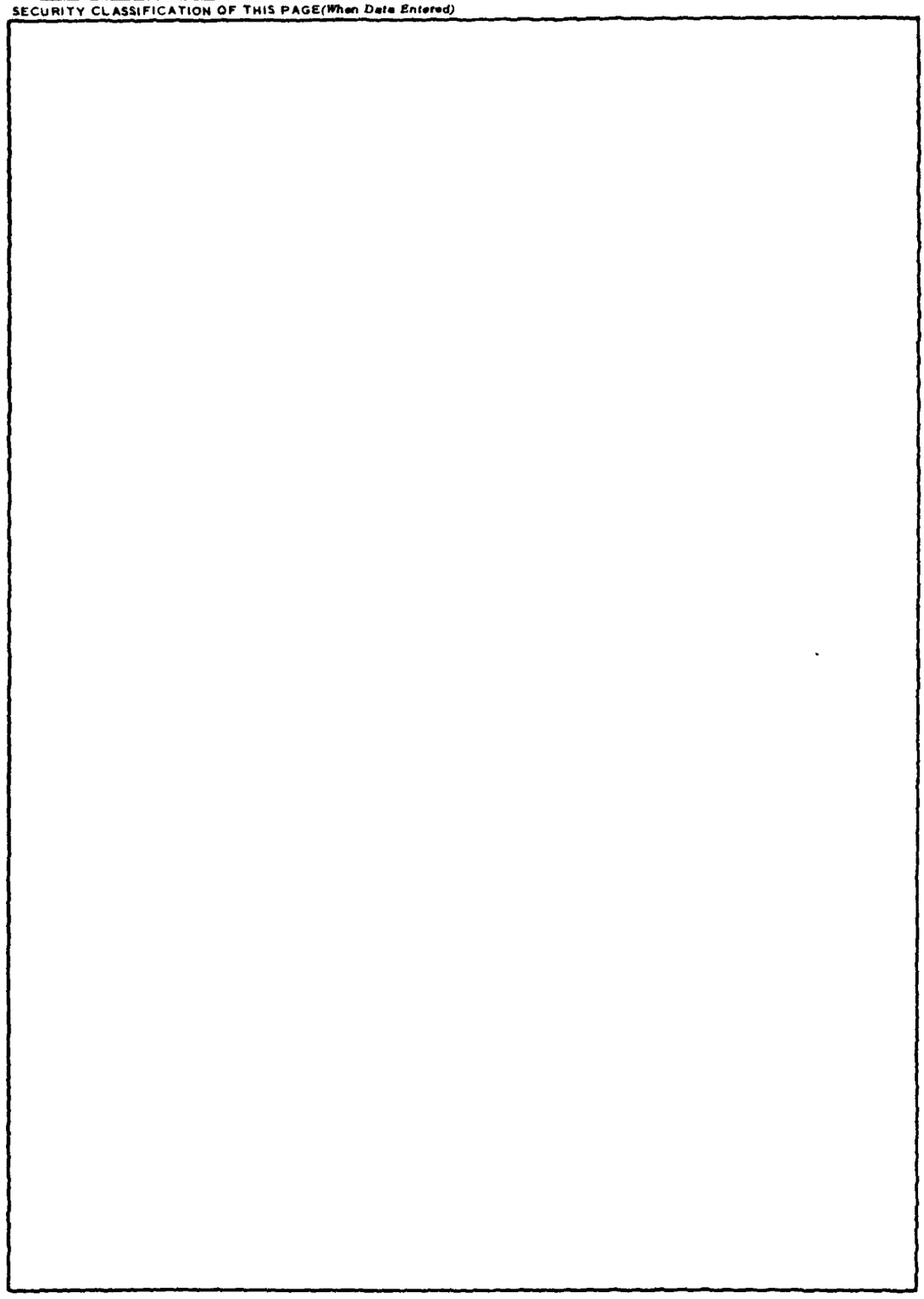

TABLE OF CONTENTS

LIST OF FIGURES

LIST OF TABLES

IMPACT OF SYSTEM ERRORS ON TMR PROCESSING

1.0 INTRODUCTION

1.1 Background and Objectives

Past efforts have demonstrated in principle how target motion resolution (TMR) techniques can be used for pinpointing the individual scattering centers on a target, such as an aircraft or a tank. The question now is what requirements are placed on the hardware quality in order to provide adequate capabilities when using these techniques in a realistic environment.

The phenomena of interest include oscillator stability, amplifier noise, system timing, and computational accuracy. Ultimately, any of these phenomena affect the radar signal processing (like TMR) through amplitude and phase errors at the input of Doppler filters. An analysis of the impact of these phenomena on TMR processing is therefore threefold. First, specifications on the phenomena, such as stability, must be transformed into equivalent amplitude and phase errors. Second, the effect of amplitude and phase errors on Doppler filter quality (resolution, sidelobe level, etc.) must be determined. Finally, the requirements on filter quality for adequate TMR performance must be determined.

In this report we consider the three steps in reverse order. First we consider the unique requirements of TMR (Section 1.3). Second we develop the general relationship between amplitude and phase errors and filter quality (Section 2.0). Third we cast these results into specifications on AM, PM, and FM spectra of the equipment (Section 3.0). Finally we present specific examples of practical interest in order to relate common hardware specifications to quality of the radar signal processing (Section 4.0). In general it is found that the hardware requirements are *not* severe for TMR processing.

1.2 Model for Radar

The radar is modeled as a contemporary pulse-Doppler radar as illustrated in Figure 1. The waveform is generated upon triggering from the radar control modules, then upconverted to microwave frequencies by mixing with a stable reference oscillator. The microwave waveform is then amplified and radiated through the antenna, amplified, then downconverted to i-f by mixing with the same stable reference oscillator as was used on transmission.

The sources of error that are relevant to us are the amplitude modulation (AM) and phase modulation (PM) on the c-w local oscillator, the AM and PM

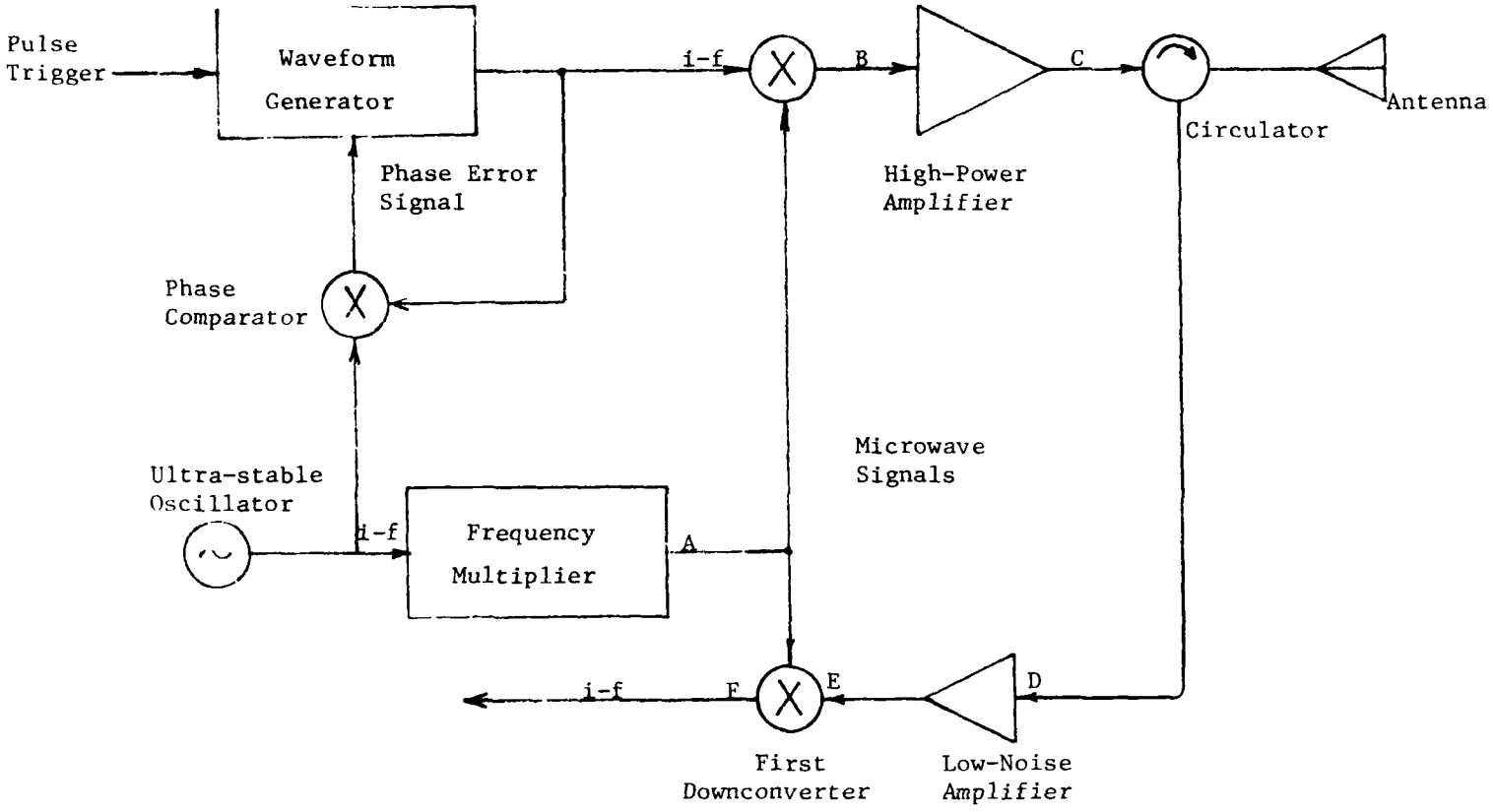

Figure 1. Model of Radar

introduced by the high-power amplifier, the time jitter of the waveform generator, the time jitter of the range tracker, and the quantization of the signal processor. Long-term (interpulse) instabilities affect mainly the quality of Doppler filtering. Short-term (intrapulse) instabilities, however, affect the quality of range compression as well.

The impact of each source of error upon filter quality is not always direct. For example, whereas the AM and PM spectra in an amplifier can be translated directly into the spectrum of a Doppler filter output, the AM and PM spectra in a local oscillator cannot. Since the same oscillator is used for both upconversion on transmission and downconversion on reception, the only relevant phase instabilities are those that arise in the time delay between transmission and return of the pulse. Notice that the starting phase of each transmitted pulse is usually controlled by a phase-locked loop so that no pulse-to-pulse phase modulations are produced by the waveform generator. On the other hand, a pulse triggering jitter is possible that will cause pulse-to-pulse amplitude modulations due to imperfect centering of a return in a range gate. In this case time jitter translates into amplitude modulation.

1.3 TMR and Doppler Filtering

Target motion resolution (TMR) is really a *generalized* form of Doppler filtering. The major generalization is that the data are phase-compensated to remove translational target motion from the data. This compensation is performed in a bootstrapping manner as illustrated in Figure 2. When performed successfully, the compensation allows one to use very long coherent integration windows, thereby leading to finer Doppler resolution than is commonly allowed. The success of the bootstrapping is ensured, however, whenever the target is observable at coarser resolutions and target translational motions are slow by comparison with the pulse repetition interval.

The phase compensation step makes TMR processing significantly different from ordinary Doppler processing in one very important way. This step corrects not only for slowly varying phases caused by motion but also for slowly varying phase errors caused by system errors. Thus, long-term phase drifts are automatically corrected. In fact, any phase errors with fluctuation periods that are less than the coherent dwell time are corrected. Typically this correction will cause a single scattering center on the target to remain

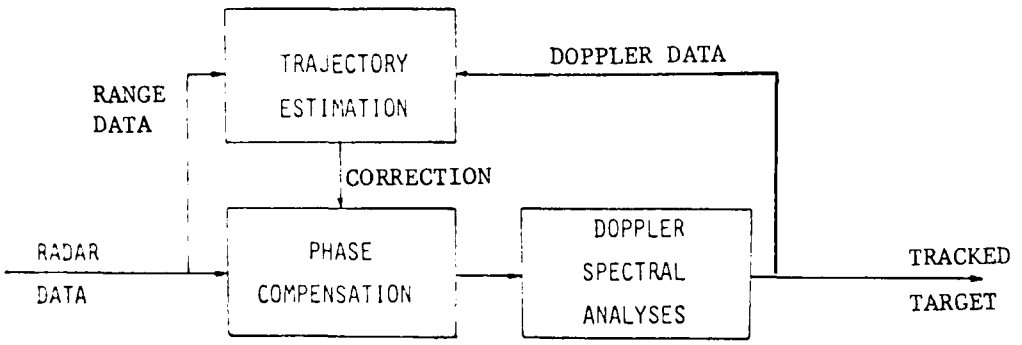

UNCLASSIFIED

Figure 2. Implementation of TMR

well-centered in a d-c Doppler filter. Any subsequent measurements on other scattering centers are therefore made *relative to* this reference scatterer Since only the physical measurement of the target scattering centers relative to each other is important for target identification, it does not really matter what compensation was required to get to this points. Whether the compensation was required because of system errors, target motion, or radar motion is irrelevant. The important point is that the success of the compensation ensures that *only high frequency error residuals remain in the data.* As a consequence there are *no* requirements on the equipment for small phase error modulations for modulation periods larger than the Doppler filtering window.

(There are special applications where the preceding statement will not apply. Suppose that we know the motion of a target so perfectly that it can be modeled with high accuracy. This will allow us to take the motion out of the data based on this model rather than data observations alone. The target will then appear stationary in the compensated data, showing only its motions about its center of gravity, as long as the radar introduces no phase errors of its own. In such an application any long-term phase drift of the equipment will remain in the motion compensated data as a residual motion. However, these applications are so rare that they deserve special consideration. The only application of this type that comes to mind is one where the launching and impact point of a missile are known very accurately, and one is additionally willing to model the effect of the atmosphere. We shall not address this specialized application here, so that for our purposes phase modulation with periods much longer than the coherent processing window are indeed irrelevant.)

The question still remains, however, what equipment characteristics are required for the bootstrapping itself to be a success. The only requirement is that the target be resolvable from its surroundings even when the coherent dwell time is limited to a time over which the residual Doppler is essentially constant. Thus there could be a problem in a very heavy clutter environment in that the integration time might be too short and the Doppler sidelobes might be too high to adequately suppress the clutter. On the other hand, since the target must be detected anyway before TMR processing is initiated, a high signal-to-clutter ratio out of the Doppler filters is already ensured.

It can therefore be stated that *no* special requirements must be met in order to initiate TMR bootstrapping, other than that the target must be detectable among the clutter.

The final question is what filter quality is required for TMR once the bootstrapping has been successfully performed. We already know that slowly varying phase errors are corrected by the phase compensation of the bootstrapping. The only remaining errors are therefore the high-frequency errors, which affect only the sidelobes. The requirement here is that when one scatterer is observed another resolvable scatterer does not interfere through excessive sidelobes. When the strongest scatterer on a target is being analyzed, Doppler sidelobe levels below -20 dB are usually enough to ensure an adequate measurement accuracy. When the weaker scatterers are being analyzed, however, deeper sidelobe levels are required to suppress the stronger scatterers so that the interference level is still 20 dB below the desired signal. Thus the sidelobe requirement depend critically on the target type and the task being performed. Generally, however, a *sidelobe level below -40 dB is adequate for practical targets and applications.*

In summary, the equipment errors need only be adequate for conventional target detection in order for TMR processing to be successfully initiated. Once TMR is properly initiated (that is, once the data are compensated for target translational motion), the only requirement is that the high-frequency errors (that is, errors with period less than the coherent dwell time) be sufficiently small that Doppler sidelobe levels can be maintained below -40 dB. In the following error analysis we therefore concentrate on the equipment requirements for ensuring low Doppler sidelobes in TMR processing.

2.0 ERROR ANALYSES

2.1 Quality of Doppler Filtering

If slowly-varying phase errors were the only type of errors introduced by the equipment then these errors would be eliminated in the trajectory compensation phase of TMR processing, and high-quality filtering would become possible. The compensated sequence of pulses for a point target would then have equal amplitudes and equal phases. After these data are weighted for low Doppler sidelobes, the input sequence would appear like Figure 3a. The frequency response of the Doppler filter would then appear like Figure 3b. This ideal filter evidently would have a narrow resolution and low sidelobes.

In actuality, however, higher-frequency errors exist in the input sequence as a result of instabilities and noise in the system. These imperfections lead directly to a degradation in filter response. Moreover, since Doppler filtering is a linear process, the filter response is the sum of the ideal response and the Fourier transform of the error voltages, as illustrated in Figure 4. Evidently the sidelobe response, which is the only response of interest to us for TMR, is dominated by the error voltages, since the sidelobes of the error-free response are adequately low by design. We are therefore justified in analyzing only the sidelobes produced by the error voltages. Our analysis approach is a Fourier analysis, since the filter output is the Fourier transform of the input. The symbols defined in Table 1 are used throughout this analysis.

The quality of the system is determined by analyzing the Doppler filter outputs for the case when an isolated, motion-compensated point target is the only reflector in the view of the radar. The input to the Doppler filter will then be, for the m-th pulse,

$$v(m) = v_o + v_e(m) \tag{1}$$

where v_o is a constant complex voltage. The Doppler response of a bank of filters to this input will just be the Fourier transform of this input, or

$$V(f) = \sum_{m=-M}^{M} v(m) e^{-j2\pi fm/f_r} \tag{2}$$

where all symbols are defined in Table 1. The sidelobe level at frequency f, which is the only quality criterion of interest to us, is

(a) Sequence of Pulses

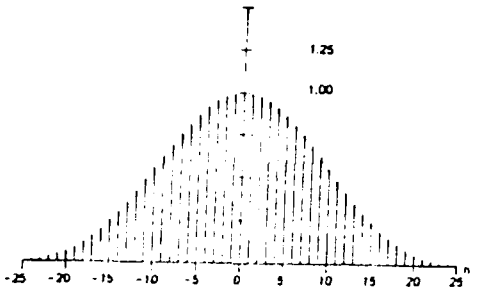

(b) Filter Frequency Response

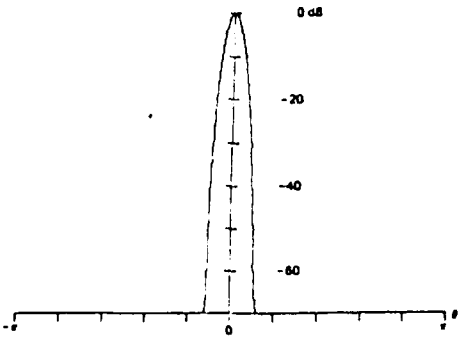

Figure 3. Ideal Doppler Filter

(a) Sequence of Pulses

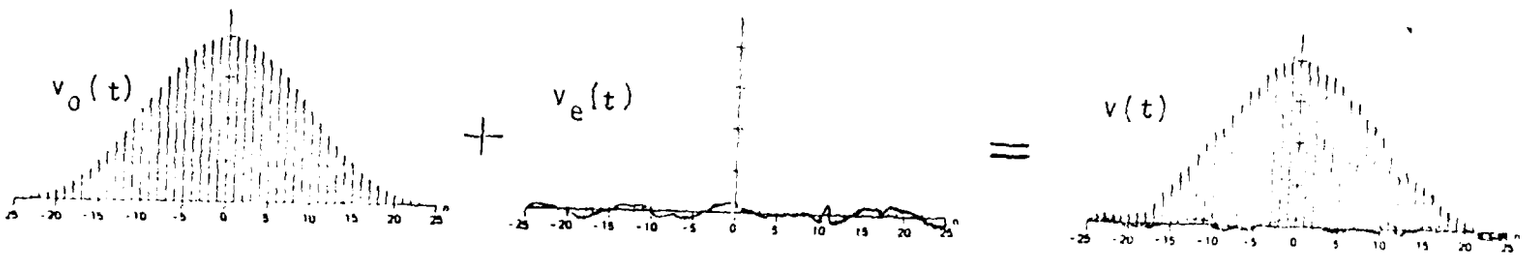

(b) Filter Frequency Response

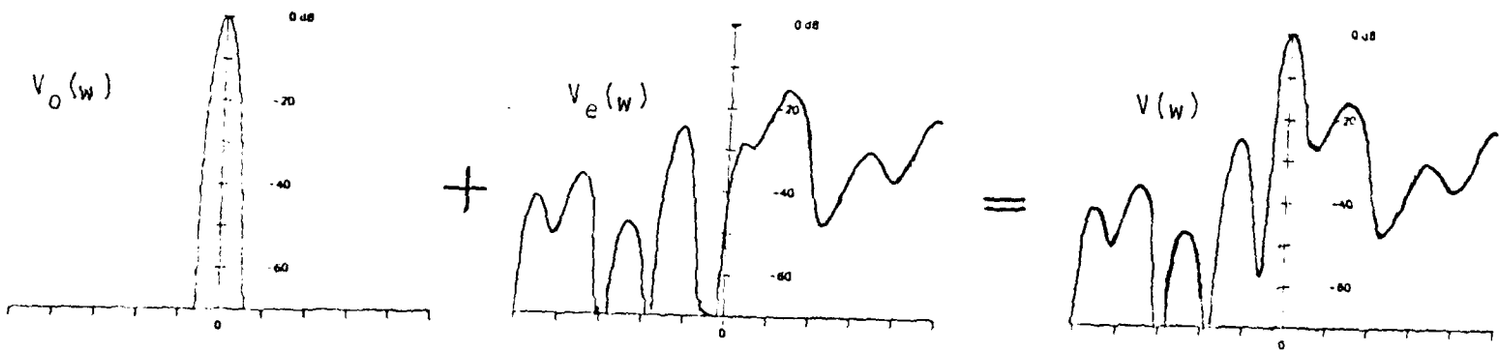

Figure 4. The Real World

Table 1. Definition of Symbols

Symbol	Formula	Description
$v(m)$		total filter input for point target
$v_e(m)$		error-only input to filter
v_o	$v(m) - v_e(m)$	constant, error-free input to filter
f		Doppler frequency relative to the point target
f_r		pulse repetition frequency of the radar
N		total number of pulses used by the filter
M	$(N-1)/2$	number of pulses past central pulse
$V(f)$		Doppler response to point target at zero Doppler
T	N/f_r	dwell time of filter
$S(f)$	$\lvert V(f)/V(0)\rvert^2$	sidelobe power level at frequency f
$a(m)$		relative amplitude error at m^{th} pulse
$\phi(m)$		phase error at m^{th} pulse
$A(f)$	eqn (11)	complex spectrum of amplitude errors
$\Phi(f)$	eqn (12)	complex spectrum of phase errors
ε_p		p-th spectral coefficient of amplitude errors
δ_p		p-th spectral coefficient of phase errors
B_o		bandwidth with which noise spectrum is measured
β_p		p-th spectral coefficient of FM error
τ_d	$2R/c$	round-trip time delay to range R
$P(f)$		spectral power at frequency f
B		pulse bandwidth

$$S(f) = \left| \frac{V(f)}{V(0)} \right|^2 \tag{3}$$

where the sidelobe region is defined as the frequencies *not* included in the intervals

$$(mf_r - \frac{1}{T}) \text{ to } (mf_r + \frac{1}{T}) \text{ for all integers m.}$$

Our analyses are based on a small error assumption, since we will accept only relatively low sidelobes. As a result we will find that (3) is rather simply related to the errors. We may rewrite (1) as

$$v(m) = v_o[1 + a(m)]e^{j\phi(m)} \tag{4}$$

where a(m) and $\phi(m)$ are the relative amplitude and phase errors. Then for small errors we have

$$v(m) \cong v_o + v_o a(m) + jv_o\phi(m) \tag{5}$$

Moreover, since the error-free term dominates the filter response in the mainlobe and the error-only terms dominate in the sidelobe region, the sidelobe level of interest can be written from (3) and (5) as

$$S(f) = |A'(f) + j\Phi'(f)|^2 \tag{6}$$

where A'(f) and $\Phi'(f)$ are the sidelobe response caused by the amplitude errors and phase errors, respectively, and are defined from (2) as

$$A'(f) = \sum_{m=-M}^{M} a(m)e^{-j2\pi fm/f_r} \tag{7}$$

$$\Phi'(f) = \sum_{m=-M}^{M} \phi(m)e^{-j2\pi fm/f_r} \tag{8}$$

The problem now is to determine the responses A'(f) and $\Phi'(f)$ in terms of some commonly specified descriptions of the system errors which result in the errors a(m) and $\phi(m)$ at the filter input. The method of determing these responses depends on the type of error being analyzed. For most errors, such as

those caused by AM and PM noise in the transmitting amplifier, or those caused by inadequate quantization in the radar signal processor, the determination is direct. That is, the AM and PM spectra of the error noise become the Doppler responses of the filters, except that the spectra are folded into a single PRF interval. This case is analyzed first. For some errors, however, such as those introduced by the local oscillator that is common to both the transmitter and receiver, the errors are partially cancelled before the Doppler filter inputs. For these errors one must examine the radar implementation and compute the error residuals from a combination of the AM and PM spectra of the original errors *and* a knowledge of the way in which errors are cancelled. This case is considered second.

In either case we need a convenient description of the error spectrum of the hardware device in question. The most convenient approach for both random and deterministic errors is a Fourier description of the spectrum. Suppose the AM and PM errors are the continuous functions $a(t)$ and $\phi(t)$, with AM and PM spectra $A(f)$ and $\Phi(f)$. We do *not* require a very fine knowledge of these spectra because our observation time is limited. That is, if the TMR dwell time is T, then we need specify the spectra at intervals no finer than 1/T. In fact, the errors can be expanded in a Fourier series over the observation time as

$$a(t) = \sum_{p=-\infty}^{\infty} \varepsilon_p e^{jp2\pi t/T} \tag{9}$$

$$\phi(t) = \sum_{p=-\infty}^{\infty} \delta_p e^{jp2\pi t/T} \tag{10}$$

and the corresponding *observable* spectra are

$$A(f) = \sum_{p=-\infty}^{\infty} \varepsilon_p \frac{\sin \pi(fT + p)}{\pi(fT + p)} \tag{11}$$

$$\Phi(f) = \sum_{p=-\infty}^{\infty} \delta_p \frac{\sin \pi(fT + p)}{\pi(fT + p)} \tag{12}$$

The coefficients ε_p and δ_p are therefore just samples of the spectra at frequencies

$$f_p = p/T \tag{13}$$

as seen through a filter of bandwidth $1/T$. These coefficients can usually be determined from a knowledge of the spectrum as seen through some other bandwidth B_o. When the spectrum is deterministic and only a single spectral line is passed through the filter, the same spectral values can be used for both bandwidths. When the spectrum is random, on the other hand, the noise *power* to be used for the Fourier coefficients in (11) and (12) must be reduced in the ratio $1/B_oT$.

2.2 Amplifier and Processor Errors

Amplifier and processor errors are not partially cancelled on reception. Consequently the AM and PM spectra for these components can be translated almost directly into the Doppler sidelobe characteristics. The only subtlety is the effect of sampling. The errors can be written from (9) and (10) as

$$a(m) = \sum_{p=-\infty}^{\infty} \varepsilon_p e^{jp2\pi m/N} \tag{14}$$

$$\delta(m) = \sum_{p=-\infty}^{\infty} \delta_p e^{jp2\pi m/N} \tag{15}$$

But because of the uniform sampling provided by the pulse train these errors can also be written as

$$a(m) = \sum_{p=-M}^{M} \varepsilon'_p e^{jp2\pi m/N} \tag{16}$$

$$\phi(m) = \sum_{p=-M}^{M} \delta'_p e^{jp2\pi m/N} \tag{17}$$

where

$$\varepsilon_p' = \sum_{q=-\infty}^{\infty} \varepsilon_{p+qN} \tag{18}$$

$$\delta_p' = \sum_{q=-\infty}^{\infty} \delta_{p+qN} \tag{19}$$

These newly defined coefficients can now be related very directly to the sidelobe level of interst.

From (6) we recall that the sidelobe level caused by AM is $|A'(f)|^2$ and the sidelobe level caused by PM is $|\Phi'(f)|^2$. From (6), (7), (16), and (17), these spectra can be written

$$|A'(f)|^2 = \left| \sum_{p=-M}^{M} \varepsilon_p' \frac{\sin \pi N(\frac{p}{N} - \frac{f}{f_r})}{\pi(\frac{p}{N} - \frac{f}{f_r})} \right|^2 \tag{20}$$

$$|\Phi'(f)|^2 = \left| \sum_{p=-M}^{M} \delta_p' \frac{\sin N(\frac{p}{N} - \frac{f}{f_r})}{\pi(\frac{p}{N} - \frac{f}{f_r})} \right|^2 \tag{21}$$

For all practical purposes the only terms in the sum that contribute to the result are the terms for p near

$$p \approx fN/f_r = fT \tag{22}$$

Thus, the sidelobe level for a Doppler frequency f in the interval

$$\frac{p - 1/2}{T} < f < \frac{p + 1/2}{T} \tag{23}$$

is given approximately by ε_p' or δ_p' alone.

Thus we have the results for AM that

$$S(f) = |A'(f)|^2 \approx |\varepsilon'_p|^2 = \left| \sum_{q=-\infty}^{\infty} \varepsilon_{p+qN} \right|^2 \tag{24}$$

where

$$p = \text{INT}\ (fT + \tfrac{1}{2}) \tag{25}$$

Similarly, we have the result for PM that

$$S(f) = |\Phi'(f)|^2 \approx |\delta'_p|^2 = \left| \sum_{q=-\infty}^{\infty} \delta_{p+qN} \right|^2 \tag{26}$$

The Doppler sidelobe level at any frequency is therefore found directly from the AM or PM spectrum (as described by the spectral samples ε_p and δ_p) merely by folding the entire spectrum onto a single PRF interval.

PM spectra are often specified via FM spectra. In this case the spectral values of the FM must first be translated into the spectral values of the PM, and then into the Doppler sidelobe levels in accordance with (26). Suppose the FM is defined in terms of the PM as

$$f(t) = \frac{1}{2\pi} \frac{d}{dt} \phi(t) \tag{27}$$

and we expand the FM into a Fourier series over the observation interval as

$$f(t) = \sum_{p=-\infty}^{\infty} \beta_p \, e^{jp2\pi t/T} \tag{28}$$

where, from (27) and (10),

$$\beta_p = \delta_p \, p/T \tag{29}$$

The Doppler sidelobe level from FM is therefore, from (27) and (26),

$$S(f) = |\Phi'(f)|^2 \approx \left| \sum_{q=-\infty}^{\infty} \frac{T}{p+qN} \, \delta_{p+qN} \right|^2 \tag{30}$$

So far we have inherently assumed a deterministic error in that we have implied that (24), (26), and (30) are specific, constant sidelobe levels. When the errors are random, however, we can only talk about an average sidelobe level $<S(f)>$. Similarly, the noise spectra will be measured as average power levels with the coefficients $<|\varepsilon_p|^2>$, $<|\delta_p|^2>$, and $<|\beta_p|^2>$ for the three types of modulation. The corresponding results for noise modulations follow from the deterministic results (24), (26), and (30) by evaluating the averages and recognizing all coefficients are uncorrelated with each other. These results, along with the previously detailed deterministic results, are summarized in the top half of Table 2.

2.3 Oscillator Errors

The characteristics of the stable local oscillator that are common to the transmitter and receiver are less directly translated into Doppler sidelobes. It is only the *residual* modulations after the first downconversion in the receiver that affect the Doppler filters. The output of the oscillator can be written as

$$s(t) = s_o[1 + \tilde{a}(t)]e^{j\tilde{\phi}(t)} \tag{31}$$

where $\tilde{a}(t)$ and $\tilde{\phi}(t)$ are the spurious or random modulations to be analyzed. Upon reception this signal is mixed with the radar return which itself involves a time-delayed replica of the oscillator signal. The input to the signal processor is therefore, ignoring the pulse modulation for the moment,

$$v(t) = s(t)\, s^*(t - \tau_d) \tag{32}$$

where the round-trip time delay τ_d is defined as

$$\tau_d = 2R/c \tag{33}$$

With a small-error approximation the input to the signal processor becomes

$$v(t) = s_o^2 + s_o^2[\tilde{a}(t) + \tilde{a}(t - \tau_d)] + j s_o^2[\tilde{\phi}(t) - \tilde{\phi}(t - \tau_d)] \tag{34}$$

where the first term is the usual error-free term, the second term is the AM term, and the third term is the PM or FM term.

Table 2. Sidelobe Power Level at Frequency f = p/T in Terms of Fourier Coefficients

Component	Type	AM	PM	FM
Amplifier	Spurious	$\left\lvert \sum_{q=-\infty}^{\infty} \varepsilon_{p+qN} \right\rvert^2$	$\left\lvert \sum_{q=-\infty}^{\infty} \delta_{p+qN} \right\rvert^2$	$\left\lvert \sum_{q=-\infty}^{\infty} \frac{T}{p+qN} \beta_{p+qN} \right\rvert^2$
	Noise	$\sum_{q=-\infty}^{\infty} \langle \lvert \varepsilon_{p+qN} \rvert^2 \rangle$	$\sum_{q=-\infty}^{\infty} \langle \lvert \delta_{p+qN} \rvert^2 \rangle$	$\sum_{q=-\infty}^{\infty} \left(\frac{T}{p+qN} \right)^2 \langle \lvert \beta_{p+qN} \rvert^2 \rangle$
Oscillator	Spurious	$\left\lvert \sum_{q=-\infty}^{\infty} \varepsilon_{p+qN} [1+e^{-j(p+qN)2\pi\tau_d/T}] \right\rvert^2$	$\left\lvert \sum_{q=-\infty}^{\infty} \delta_{p+qN} [1-e^{-j(p+qN)2\pi\tau_d/T}] \right\rvert^2$	$\left\lvert \sum_{q=-\infty}^{\infty} \frac{T}{(p+qN)} \beta_{p+qN} [1-e^{-j(p+qN)2\pi\tau_d/T}] \right\rvert^2$
	Noise	$4 \sum_{q=-\infty}^{\infty} \langle \lvert \varepsilon_{p+qN} \rvert^2 \rangle \cos^2 \frac{(p+qN)\pi\tau_d}{T}$	$4 \sum_{q=-\infty}^{\infty} \langle \lvert \delta_{p+qN} \rvert^2 \rangle \sin^2 \frac{(p+qN)\pi\tau_d}{T}$	$\sum \frac{4T^2}{(p+qN)^2} \langle \lvert \beta_{p+qN} \rvert^2 \rangle \sin^2 \frac{(p+qN)\pi\tau_d}{T}$

The relevant sidelobe levels are found from (6), (7), and (8) where the modulations are now

$$a(m) = \tilde{a}(m/f_r) + \tilde{a}\left(\frac{m}{f_r} - \tau_d\right) \tag{35}$$

$$\phi(m) = \tilde{\phi}(m/f_r) - \tilde{\phi}\left(\frac{m}{f_r} - \tau_d\right) \tag{36}$$

The underlying oscillator spectra are analyzed by Fourier series as in (9) and (10), whereas the above sampled coefficients are analyzed as in (16) and (17). Following the outlined formalism we find that (20) and (21) are still valid, but with

$$\varepsilon_p' = \sum_{q=-\infty}^{\infty} \varepsilon_{p+qN} \left[1 + e^{-j(p+qN)2\pi\tau_d/T}\right] \tag{37}$$

$$\delta_p' = \sum_{q=-\infty}^{\infty} \delta_{p+qN} \left[1 - e^{-j(p+qN)2\pi\tau_d/T}\right] \tag{38}$$

where ε_p and δ_p are the spectral coefficients for the oscillator modulations $\tilde{a}(t)$ and $\tilde{\phi}(t)$. Similarly, the results for FM spectra are analogous to (38). Thus we have, for deterministic signals, the sidelobe levels given by (24), (26), and (30), except that the Fourier coefficients are redefined by (37) and (38).

The precise results are listed in Table 2 for spurious oscillator signals. The situation for noise modulations can be handled, as before, by evaluating average powers from the deterministic formulas. These results are also summarized in Table 2.

2.4 Practical Application of Results

Meaning of the Fourier Coefficients

The results in Table 2 are totally general but are not easily used in their present form. In order to translate these results into practically useful results based on commonly specified measurements we must first understand

what the Fourier coefficients in Table 2 actually represent. If we write the error-prone signal explicitly in terms of the carrier, AM, PM, and FM components then we have

$$s(t) = s_o(t)\ [1 + a(t)][e^{j\phi(t)}][e^{j2\pi tf(t)}] \qquad (39)$$

where the error-free component is

$$s_o(t) = s_o e^{j2\pi f_c\ t}$$

for a carrier frequency f_c, and the error modulations $a(t)$, $\phi(t)$, and $f(t)$ are all real functions.

The Fourier analyses defined in (9), (10), and (26) are just the infinite Fourier series expansions of the respective modulations in (39) over a time interval of duration T. As a consequence the Fourier coefficient ε_p for AM is just the output of a filter of bandwidth 1/T centered at frequency p/T relative to d-c. (For the *total* signal s(t), and assuming negligible PM and FM, the coefficient ε_p is also the relative output of the same filter centered at frequence p/T relative to the carrier frequency.) Similarly, the coefficients for PM and FM, δ_p and β_p, are outputs of filters for which $\phi(t)$ and $f(t)$ are the inputs rather than $a(t)$.

The numerical units of the coefficients depend on the type of modulation. For AM the error function is evidently normalized to unity amplitude. The Fourier coefficients are therefore amplitudes relative to the carrier amplitude. AM power spectra are, in fact, typically specified in units of dB below the carrier. For PM the error function has the units of radians relative to the carrier phase. Since errors of interest to us are small, this phase error function can be visualized as a complex amplitude function, or

$$e^{j\phi(t)} \approx 1 + j\phi(t)$$

and $\phi(t)$ in radians can now be thought of as a complex amplitude relative to the carrier amplitude. Consequently, PM power spectra are also typically specified in units of dB below the carrier power. For FM however, the units are less well-standardized.

The FM error function f(t) is measured in Hz so that the Fourier coefficients are also measured in Hz. The Fourier coefficient β_p is therefore the amplitude of the frequency deviation as seen through a filter of bandwidth 1/T centered at frequency p/T. For example, if the FM is just a sinusoidal FM of peak-to-peak frequency deviation Δf and modulating frequency $f_m = p/T$, then the Fourier coefficient β_p is just $\Delta f/2$ and all other coefficients are zero. FM spectra are typically specified, however, in some normalized fashion rather than in Hz for Δf alone. Unfortunately, there is no universal standard for this normalization. The FM power spectrum is variously defined as a dimensionless power ratio relative to the pulse bandwidth B, modulating frequency f_m, or carrier frequency f_c, and the spectrum is therefore measurable in units of dB. In order to avoid confusion we will always describe the FM spectrum in terms of the dimensioned quantities: Hz for the Fourier coefficients and $(Hz)^2$ for the spectral powers.

Sidelobe Response for a Single Spurious Signal

When the only error source is a single sinusoidal signal, the sidelobe response can be determined directly. (The results can also be found from Table 2 for the case where the modulating frequency is an integer multiple of 1/T.) For example, if we represent the sinusoidal modulation function as g(t) (whether it be AM, PM, or FM) and the peak-to-peak sine-wave amplitude as Δg, then we may write the real modulation function as

$$g(t) = (\Delta g/2)\cos(2\pi f_m t + \phi_m) = g_o e^{j2\pi f_m t} + g_o^* e^{-j2\pi f_m t} \qquad (40)$$

where

$$g_o = e^{j\phi_m}\,\Delta g/4 \qquad (41)$$

We therefore have spectral components of the modulation function at frequencies $+f_m$ and $-f_m$ relative to d-c, with amplitude-squared (or "power") values of

$$P(f_m) = P(-f_m) = |g_o|^2 = (\Delta g)^2/16 \qquad (42)$$

When the spurious signal originates in an amplifier rather than the common L.O., these results can be applied directly. For example, for AM and PM we recall that the spectrum observed out of the digital Doppler filters is a folded version of the continuous spectrum, and has spectral widths 1/T corresponding

to the filter duration T. As a consequence, the Doppler filters have sidelobe peaks at $\hat{f} = \pm f_m$ where f lies in the range $-f_r/2$ to $+ f_r/2$ and

$$\hat{f}_m = [(f_m + f_r/2) \text{ modulo } (f_r)] - f_r/2 \tag{43}$$

and the actual sidelobe responses are

$$S(f) \tilde{=} P(f_m) \left\{ \left| \frac{\sin \pi(f-f_m)T}{\pi(f-\hat{f}_m)T} \right|^2 + \left| \frac{\sin \pi(f+\hat{f}_m)T}{\pi(f+\hat{f}_m)T} \right|^2 \right\} \tag{44}$$

The peak sidelobe level is therefore

$$S(\pm \hat{f}_m) = P(\pm f_m) \tag{45}$$

For FM the peak response depends on the modulation frequency f_m as well as the power $P(f_m)$. By analogy with Table 2 the peak sidelobe level is

$$S(\pm \hat{f}_m) = P(\pm f_m)/f_m^2 \tag{46}$$

When the spurious signal originates in the common L.O., so that the phase errors are partially cancelled on reception the results in (45) for AM and PM and (46) for FM are modified by the cancellation factor that is evident in Table 2. Following the same argument as above we now have for the peak sidelobe levels the responses at $f = \hat{f}_m$, which are

$$\left.\begin{aligned} S(\pm \hat{f}_m) &= P(\pm f_m)\ 4 \cos^2(\pi\tau_d f_m) \text{ for AM} \\ S(\pm \hat{f}_m) &= P(\pm f_m)\ 4 \sin^2(\pi\tau_d f_m) \text{ for PM} \\ S(\pm \hat{f}_m) &= P(\pm f_m)\ 4 \sin^2(\pi\tau_d f_m)/f_m^2 \text{ for FM} \end{aligned}\right\} \tag{47}$$

where $P(f_m)$ is defined in terms of the peak-to-peak amplitude of the respective modulation function in accordance with (42). That is,

$$\left.\begin{aligned} P(f_m) &= (\Delta a)^2/16 \text{ for AM (dimensionless)} \\ P(f_m) &= (\Delta\phi)^2/16 \text{ for PM (radians-squared)} \\ P(f_m) &= (\Delta f)^2/16 \text{ for FM (Hertz-squared)} \end{aligned}\right\} \quad (48)$$

and Δa, $\Delta\phi$, Δf are the peak-to-peak amplitudes of $a(t)$, $\phi(t)$, and $f(t)$, which are used in (39).

These results are summarized in Table 3.

Sidelobe Response for a Noisy Signal

When the error source is random noise, a large number of Fourier coefficients are involved. If the system bandwidth is B then all Fourier coefficients are involved that lie in the range

$$-BT \leq p \leq BT \quad (49)$$

The *total* noise power is the sum of powers for all coefficients in this range. However, the coefficients are filter outputs for a filter width of 1/T. Thus, if the available noise spectrum is measured in a bandwidth B_o, then the coefficients have a power that is changed by the ratio $1/B_oT$ relative to the measured spectral powers.

Specifically, let us define $P_o(f)$ as the spectral power measured for the modulation of interest in a band of bandwidth B_o. Then the p^{th} Fourier coefficient for that modulation is the re-normalized power at frequency $f = p/T$, or

$$P_o(p/T)/B_oT \quad (50)$$

The sidelobe level at a frequency $f = p/T$ then follows from Table 2 for the various cases, where (50) replaces the amplitude-squared of the coefficient, remembering that the different coefficients are uncorrelated so that only these spectral powers are relevant.

For example, the AM noise produces a sidelobe at frequency $f = p/T$ of

$$S(p/T) = \left| \sum_{q=-\infty}^{\infty} \varepsilon_{p+qN} \right|^2 = \sum_{q=-\infty}^{\infty} \left| \varepsilon_{p+qN} \right|^2$$

$$= \sum_{q=-\infty}^{\infty} P_o\left(\frac{p+qN}{T}\right)/B_oT \quad (51)$$

Table 3. Power Sidelobe Level at Doppler Frequency f

Component	Type	AM	PM	FM
Amplifier	Spurious	$P(f_m)\ S_o(f,\ f_m,\ -f_m)$	$P(f_m)\ S_o(f,\ f_m,\ -f_m)$	$\frac{P(f_m)}{f_m^2}\ S_o(f,\ f_m,\ -f_m)$
	Noise	$\frac{1}{B_o T}\sum_{q=-\infty}^{\infty} P_o(f+qf_r)\ S_o(f,f_1,f_2)$	$\frac{1}{B_o T}\sum_{q=-\infty}^{\infty} P_o(f+qf_r)\ S_o(f,f_1,f_2)$	$\frac{1}{B_o T}\sum_{q=-\infty}^{\infty} \frac{P_o(f+qf_r)}{(f+qf_r)^2}\ S_o(f,f_1,f_2)$
Oscillator	Spurious	$4P(f_m)\cos^2(\pi\tau_d f_m)\ S_o(f,\hat{f}_m,-\hat{f}_m)$	$4P(f_m)\sin^2(\pi\tau_d f_m)\ S_o(f,\hat{f}_m,-\hat{f}_m)$	$\frac{4P(f_m)}{f_m^2}\sin^2(\pi\tau_d f_m)\ S_o(f,\hat{f}_m,-\hat{f}_m)$
	Noise	$\frac{4}{B_o T}\sum_{q=-\infty}^{\infty} P_o(f+qf_r)\ S_o(f,f_1,f_2)\cos^2[\pi\tau_d(f+qf_r)]$	$\frac{4}{B_o T}\sum_{q=-\infty}^{\infty} P_o(f+qf_r)\ S_o(f,f_1,f_2)\sin^2[\pi\tau_d(f+qf_r)]$	$\frac{4}{B_o T}\sum_{q=-\infty}^{\infty} \frac{P_o(f+qf_r)}{(f+qf_r)^2}\ S_o(f,f_1,f_2)\sin^2[\pi T_d(f+qf_r)]$

Definitions: $S_o(f,g,h) = \left|\frac{\sin \pi(f-g)T}{\pi(f-g)T}\right|^2 + \left|\frac{\sin \pi(f-h)T}{\pi(f-h)T}\right|^2$

$f_1 \triangleq \text{INT}(fT)/T$

$f_2 \triangleq \text{INT}(1+fT)/T$

$f_m = -\frac{f_r}{2} + (f_m + f_r/2) \text{ modulo } f_r$

$\tau_d = 2R/c$ where R is range to target

f_r = pulse repetition frequency of radar

B_o = measurement bandwidth for noise modulation

f_n = modulation frequency for spurious modulation

In terms of the frequency f and the PRF f_r, this result is

$$S(f) = \sum_{q=-\infty}^{\infty} P_o(f + qf_r)/B_oT \tag{52}$$

At frequencies for which fT is *not* an integer, however, the expression is more complex and must include the filter shape. In this more general case we have

$$S(f) = \sum_{p=-\infty}^{\infty} \sum_{q=-\infty}^{\infty} \frac{P_o(f + qf_r)}{B_oT} \left| \frac{\sin \pi(f - \frac{p}{T})}{\pi(f - \frac{p}{T})} \right|^2 \tag{53}$$

where f lies in the range $-f_r/2$ to $+f_r/2$. For all practical purposes, the only terms in p that contribute to the sum are those for which $|f - p/T| < 1/T$. Thus we may generally write

$$S(f) \cong \sum_{l=-\infty}^{\infty} \left[\frac{P_o(f + qf_r)}{B_oT}\right] \left\{ \left| \frac{\sin \pi(f - f_1)T}{\pi(f - f_1)T} \right|^2 + \left| \frac{\sin \pi(f - f_2)T}{\pi(f - f_2)T} \right|^2 \right\} \tag{54}$$

where

$$f_1 = \text{INT}(fT)/T$$

$$f_2 = \text{INT}(1 + fT)/T$$

The result (54) also obtains for the PM case of a noisy amplifier. The FM case is modified only by a $1/(f + qf_r)^2$ factor. For noise in a common L.O., analogous results are obtained but with the factor that represents partial cancelation, as given in Table 2, included. The various results for all cases are summarized in Table 3.

Practical Use of Results

The results given in Table 3 may be used *directly* from specified spectra. All quantities except for the powers P(f) and $P_o(f)$ are defined in the table. The only remaining clarification needed is the evaluation of the powers P(f) and $P_o(f)$.

The power P(f) for a spurious signal is half the mean-square amplitude of the modulation, as described in (40) through (42). In terms of the peak-to-peak

amplitude of the modulation, the power is 1/16th of the square of this amplitude. Thus

$$\left.\begin{aligned} P(f_m) &= (\Delta a)^2/16 \text{ for AM} \\ P(f_m) &= (\Delta\phi)^2/16 \text{ for PM} \\ P(f_m) &= (\Delta f)^2/16 \text{ for FM} \end{aligned}\right\} \tag{55}$$

where the peak-to-peak modulation amplitudes are

$$\left.\begin{aligned} &\Delta a \text{ for AM, in amplitude relative to carrier} \\ &\Delta\phi \text{ for PM, in radians} \\ &\Delta f \text{ for FM, in Hertz} \end{aligned}\right\} \tag{56}$$

The power $P_o(f)$ for a noise signal is the average power measured in a bandwidth B_o, and has units that are consistent with (55) and (56). When the noise has a flat spectrum over a bandwidth B, the noise is often specified by a single variance σ_n^2 rather than the entire spectrum. In that case the power to be used in Table 3 is

$$P_o(f) = \begin{cases} \sigma_N^2 \, B_o/2B \text{ for } |f| < B \\ \\ 0 \text{ otherwise} \end{cases} \tag{57}$$

3.0 SPECIFIC EXAMPLES

Virtually any error sources can be translated into spectral errors so that the results in Tables 2 and 3 can be used to determine Doppler sidelobe levels. Some applications of these results for common errors in modern radars are illustrated here.

3.1 Spurious L.O. Signals

For a first example consider a spurious FM oscillation in the L.O. at a frequency f from the carrier with frequency deviation Δf. From (55) and Table 3, the peak sidelobe level produced by this modulation is

$$\boxed{S(f) = (\pi \tau_d \Delta f/2)^2} \tag{58}$$

Thus, if the radar range is 10 km, so that the round-trip time delay τ_d is 66.7 μsec, then a peak-to-peak frequency deviation of 100 Hz will produce a sidelobe level of -39.6 dB, which is good, but now always adequate in some environments.

Expressed another way, the allowable frequency deviation for a single sinusoidal FM is

$$\Delta f \leq 2\sqrt{S(f)}/\pi\tau_d \tag{59}$$

In terms of radar range R the allowance is

$$\Delta f \leq 2c\sqrt{S}/2\pi R \tag{60}$$

Thus, for the common sidelobe specification of -40 dB, the allowance is

$$\Delta f \leq \frac{955}{R} \text{ Hz} \tag{61}$$

where range R is specified in km.

3.2 White Amplifier Noise

Suppose the power amplifier generates PM noise with a PM spectrum that is uniform over the system bandwidth B. Furthermore, suppose the noise is specified only in terms of a total noise variance σ_N^2. Then, from (57) and Table 3 the Doppler sidelobe response is

$$S(f) = \frac{1}{B_o T} \sum_{q=-Q}^{+Q} \sigma_N^2 \, B_o/2B$$

where $Q = B/f_r$. Thus

$$S(f) = \sigma_N^2/f_r T = \sigma_N^2/N \tag{62}$$

where N is the total number of pulses.

For example, if σ_N^2 is 10^{-5} (-50 dB total noise relative to the carrier) and the number of pulses is N=16, then the average sidelobe power level is -62 dB. (This noise might also be specified as a uniform -100 dB below the carrier as measured in a 1 kHz bandwidth, where the total system bandwidth is 100 MHz. The same results would be obtained as above.)

3.3 Pulse Timing Jitter

The next example involves pulse jitter in which the modulation envelope that produces high range resolution wanders from pulse to pulse. Such timing jitter can be caused by imperfect timing from the modulator or transmission or imperfect range tracking on reception. In other words, a random jitter is essentially a random time-delay mismatch between the transmitted pulse and the receiver's matched filter. This mismatch randomly changes from pulse to pulse and therefore produces an AM noise at the input to the Doppler filters. We must therefore translate a specified time jitter into the equivalent AM spectrum; then we may use the results in Table 3 to determine the resulting sidelobe level.

An adequate approximation to the effect of the random mismatch is provided by assuming a square shape for the compressed pulse. A timing error $\Delta(m)$ for the m^{th} pulse therefore produces the relative amplitude error

$$a(m) = |\Delta(m)|B \tag{63}$$

where B is the pulse bandwidth, 1/B is the pulsewidth, and $|\Delta(m)| < 1/B$.

Since the jitter is random we can only describe the effect statistically. The rms time jitter σ_T will typically be specified in seconds. The mean-square amplitude error is then

$$\langle a^2(m) \rangle = \sigma_T^2 B^2 \tag{64}$$

where the amplitude error can be expanded in the series (14). Assuming purely random jitter that is independent and statistically stationary from pulse to pulse, we can interpret this mean-square error as the total noise power for white noise, so that from (57) and Table 3, we have an average sidelobe level

$$\boxed{S(f) \tilde{=} \sigma_T^2 \, B^2/N} \tag{65}$$

for any Doppler frequency not within the mainlobe of the filter.

3.4 Colored Amplifier Noise

The final example is an amplifier with the noise spectrum illustrated in Figure 5. This is a realistic spectrum for a microwave klystron amplifier. The AM and PM noise are specified here in terms of the power in a 1 kHz band relative to the power in the carrier. Since the noise is clearly not white (that is, the same level at all frequencies) we must carefully apply the results from Table 3 taking into account the actual nonuniform spectrum. It is evident from Table 3 that the PM or AM produces a sidelobe level

$$S(f) = \frac{1}{B_o T} \sum_{n=-\infty}^{\infty} P(f + n f_r) \tag{66}$$

where P(f) is the spectral level of the PM or AM. It is further evident from Figure 5 that the PM is much stronger than the AM for our example. We are therefore justified in considering the effect of PM alone for this example.

In handling the specified noise spectrum we must recognize three distinct regions. The first region is all frequencies below 1/T where T is the dwell time of the Doppler filter being analyzed. Noise in this region has no detrimental effect on TMR processing because TMR automatically compensates for these low frequency errors. The second region is from 1/T to about 20 kHz, where the noise level falls as frequency increases. The behavior evident in Figure 5 is approximately $1/f^{1.5}$, with a level of -116 dBc at f = 2 kHz. The third region is all frequencies above 10 kHz but below the pulse bandwidth. The noise is essentially white (uniform) in this region at a level of -126 dBc.

We may now use (66) along with the spectral levels in the three regions

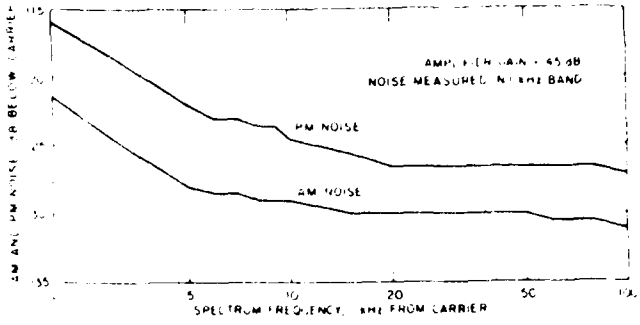

Figure 5. Typical Klystrom Amplifier Noise

to define the sidelobe level. Considering the sidelobe level at Doppler frequency f = 1/T (which is the worst case) we have

$$S\left(\frac{1}{T}\right) = \frac{P(f_o)}{B_o T} \sum_{n=-\infty}^{\infty} \left(\frac{f_o}{1/T + nf_r}\right)^{1.5} + \frac{B\, P(f_{hi})}{B_o\, f_r\, T} \qquad (67)$$

$P(f_o)$ is the level of the $1/f^{1.5}$ noise as measured at frequency f_o (e.g., $10^{-11.6}$ at f_o = 2 kHz), $P(f_{hi})$ is the level of the white noise component ($10^{-12.6}$) and B is the pulse bandwidth. For the example T = 1 second, f_r = 100 Hz, and B = 10 MHz we therefore have

$$S\left(\frac{1}{T}\right) = \frac{10^{-11.6}}{10^3} \sum_{n=-\infty}^{\infty} \left(\frac{2 \times 10^3}{1 + n\ 100}\right)^{1.5} + 10^3 \times 10^{-12.6}$$

$$= 2.25 \quad 10^{-13} \sum_{n=-\infty}^{\infty} \frac{1}{(n + .01)^{1.5}} + 10^{-9.6}$$

The infinite sum is

$$\sum_{n=-\infty}^{\infty} \frac{1}{(n + .01)^{1.5}} \approx \frac{1}{(.01)^{1.5}} + 2 \sum_{n=1}^{\infty} \frac{1}{n^{1.5}} = 1000 + 5.22$$

so that the resulting sidelobe level is

$$S\left(\frac{1}{T}\right) = 4.77 \times 10^{-10} \quad (-93.2 \text{ dB})$$

In this example the $1/f^{1.5}$ noise and the white noise contribute nearly equal total powers to this sidelobe. At higher Doppler frequencies (that is, $f \gg 1/T$) the $1/f^{1.5}$ noise falls rapidly, but the noise component of -96 dB remains as a floor to the sidelobe level. Evidently, the noise performance of a typical klystron far exceeds the requirements for low Doppler sidelobes in TMR processing.

4.0 CONCLUSIONS

In most applications of TMR the slowly-varying system errors are removed in the motion compensation phase of the processing. The only residual errors that have an important effect on performance are therefore the high-frequency errors which produce Doppler sidelobes. The level of these sidelobes can be found from a knowledge of the spectrum of the errors, as given in Table 3 for various sources of error. In general it is found that the requirements for good TMR performance are not difficult to meet with today's equipment.

(U) DISTRIBUTION

US Air Force Attn: ADTC/SD7, W. D. Hayes ADTC/SD102M, A. Smith Eglin AFB, FL 32542	1 1
US Air Force 6585th Test Group (RX) Holloman AFB, NM 88330	1
US Air Force Armament Laboratory Systems Analysis & Simulation Branch Attn: Dr. W. P. Albritton Eglin AFB, FL 32542	1
Naval Research Laboratory Systems Analysis Staff Attn: Code 5309, Dr. M. E. Tannenhaus Washington, DC 20375	1
Naval Weapons Center RF Anti-Air Branch Attn: Code 3911, Mr. M. Mumford China Lake, CA 93155	1
Naval Weapons Center Michaelson Laboratory Attn: Code 3911, Dr. G. Hewer China Lake, CA 93155	1
Naval Research Laboratory Attn: Mr. R. Gardner Washington, DC 20375	1
Pacific Missile Test Center Electromagnetic Technology Branch Code 1231 Point Mugu, CA 93042	1
Naval Air Development Center Code 60112, J. Abbasi Warminster, PA 18974	1
DRSMI-TM-E, M. Bailey	1
DRCPM-HAE, J. Cole	1
DRCPM-ROL	1
DRCPM-MD-T-T	1
DRCPM-MD-T-C	1
DRSMI-REG, Dr. Wright	15
DRSMI-RB	3
DRSMI-RPT(Record Set)	1
DRSMI-RER	1
DRSMI-REL	1
DRSMI-RE	1
DRSMI-TDR	2
DRSMI-RPR	5

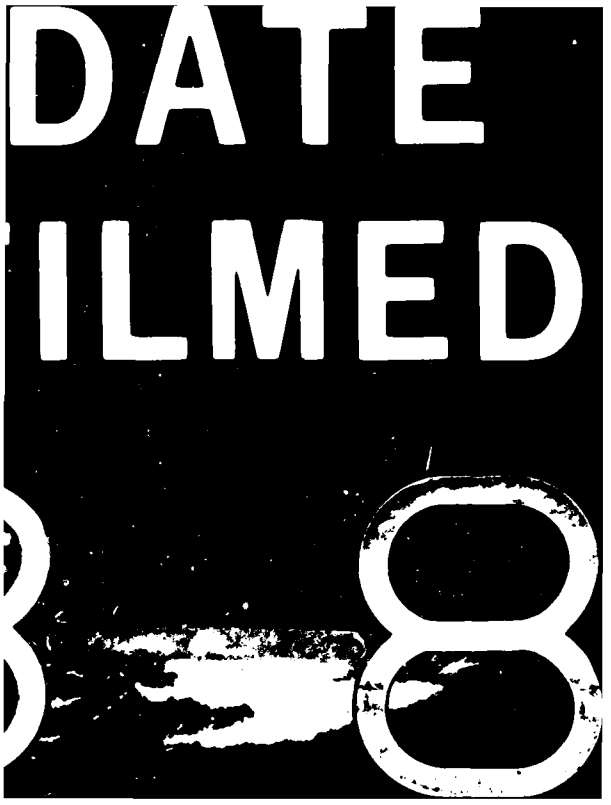
DATE
ILMED